

Supporting information for

Fluorescence enhancement of organic dyes by
femtosecond laser induced cavitation bubbles for
crystal imaging

Jiachen Yu ^{1, †}, Jianfeng Yan ^{1, †}, Lan Jiang ^{2, *}, Jiaqun Li ¹, Heng Guo ¹, Ming Qiao ¹,
Liangti Qu ³

¹ State Key Laboratory of Tribology in Advanced Equipment, Department of Mechanical
Engineering, Tsinghua University, Beijing, 100084, China

² School of Mechanical Engineering, Beijing Institute of Technology, Beijing, 100081, China

³ Department of Chemistry, Tsinghua University, Beijing, 100084, China

* Email: jianglan@bit.edu.cn

† These authors contributed equally to this work.

Pages: 13

Figures: 11

Video: 1

1. Methods

1.1 Optical setup of fluorescence enhancement in solution

Two femtosecond laser beams were used to induce fluorescence enhancement. One was used to induce the cavitation bubbles and the other was used to pump the dye solution. The 800 nm laser pulses were generated from a femtosecond laser amplifier (Conherent Elite, 800 nm, 1 kHz, 35 fs). The 400 nm laser pulses were produced from 800 nm laser by passing through the β -BaB₂O₄ (BBO) crystal and a band-pass filter. The 800 nm laser was focused into the dye solution by a long working distance 50x objective (NA 0.5). The power of the 800 nm laser was set to be 1–50 mW (1–50 μ J per pulse) to induce cavitation bubbles. The 400 nm laser was focused by a 50 mm lens. The power of the 400 nm laser range from 5 to 60 μ W (5–60 nJ per pulse). The pulse duration before focused by the objective was measured to be 50 fs by an auto correlator.

The fluorescence enhancement phenomena were studied by microscopic imaging and spectroscopy. A 10x objective (NA 0.25) was placed behind the cuvette. The focus point was projected on the sensors of the CCD camera or the spectroscopy. The optical images of the femtosecond laser induced cavitation bubbles and fluorescence emission were obtained by a CCD camera (Imaging Source DFK 237U274). The emission spectra was measured by a fiber coupled spectrometer (Oceanview USB 400). The exposure time was set to be 1 s in order to gain enough signal. Note that although the input and detection light paths in the schematics show a collinear arrangement, the light emission is not directional. The experimental setup is used to gain enough signal.

1.2 Dye solution preparation

The dye solution was prepared by dissolving dye compounds into water and ethanol. Three kinds of dye compounds with diverse fluorescent wavelengths were used in this study. 0.001% (wt.) Rhodamine B (RB), 0.001% (wt.) Rhodamine 6G (R6G), and 0.001% (wt.) Proflavin (PF) solutions were prepared individually. The dye compounds were firstly dissolved into the mixture of water and ethanol (volume ratio 1:1) at a concentration of 1% (wt.). The solution was stirred by magnetic stirrers at the speed of 300 r/min for 10 min, and then centrifuged at the speed of 10000 r/min. The

as prepared dye solution was diluted to the desired concentration by adding deionized water. The mixture of three kinds of dye solution (volume ratio R6G:RB:PF = 1:1:2) was also prepared to study the wavelength tunability of the bubble enhanced fluorescence. Two kinds of containers were used in the experiments. A 500 μm thick container was made by two pieces of cover glass with 500 μm PDMS film as spacer. In the parametric studies, 10 mm thick cuvettes were used to avoid the accumulation of bubbles on the walls of containers.

1.3 Protein crystals preparation

The hen egg white lysozyme (HEWL) was chosen to be the sample protein. The protein solution was prepared by dissolving 24 mg/mL HEWL compounds (Sigma Aldrich) into deionized water. The buffer also contains 2.5% (wt.) NaCl and 1 M NaAC which is purchased from Aladin. The solution was stirred by magnetic stirrers at the speed of 300 r/min for 10 min. The as prepared solution was then centrifuged at the speed of 10000 r/min. A sitting droplet method was applied using the crystallization plate. 96-well plates were applied and 200 μL of reservoir was added into each well. Then 5 μL of the protein solution was dripped on the crystallization plate. the protein solution was incubated with the reservoir at 23 $^{\circ}\text{C}$ with a constant temperature incubator. Protein crystals with sizes from 50 to 200 μm could be acquired in 48 hours.

2. Relationship between fluorescence emission intensity and pump laser parameters

2.1 Pump intensity

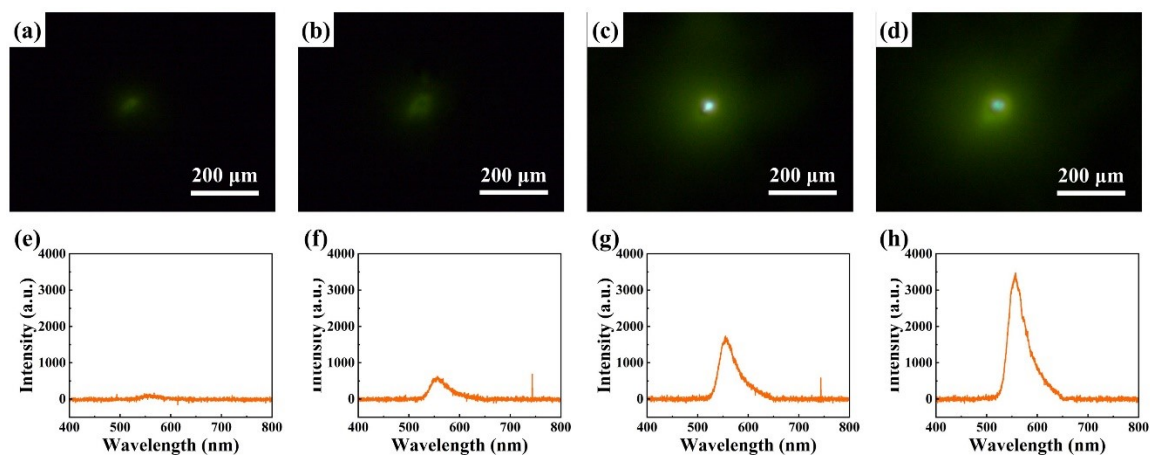


Figure S1. (a)–(d) The CCD images of femtosecond laser focused in the dye solutions. (e)–(h) The emission spectra of femtosecond laser focused in the dye solutions. The laser powers were set to be 2, 5, 10 and 20 mW. The 800 nm femtosecond laser travelled through the BBO before focusing so that the laser beam contains both the 400 nm and the 800 nm fs laser. The laser power stands for the input 800 nm laser. (See also Supporting Information **Video S1**)

2.2 Dye concentration

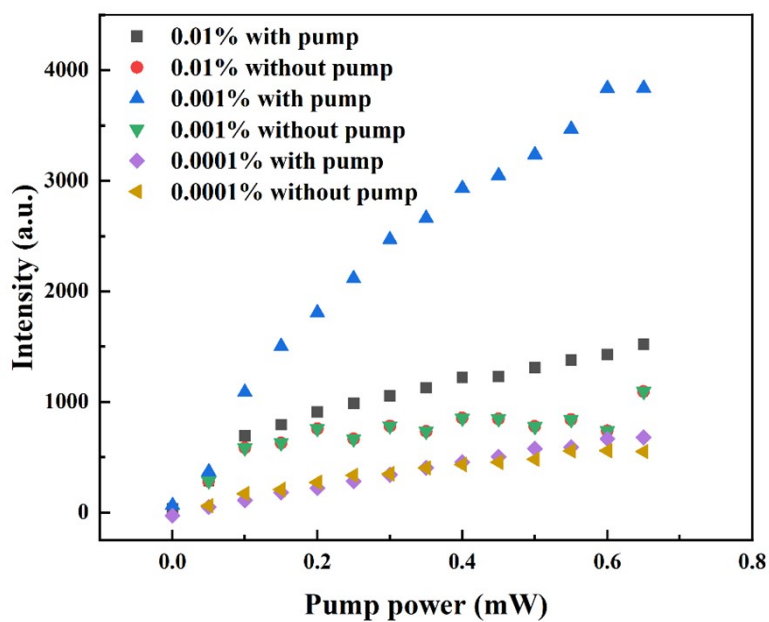


Figure S2. The relationship between peak emission intensity and the pump power at different dye concentration. The R6G was used as the fluorescent dye. The pump power refers to the power of 400 nm laser. The power of 800 nm fs laser which was used to generate cavitation bubbles was 20 mW. 0.001% (wt) R6G solutions shows the highest emission intensity.

2.3 Pulse delay

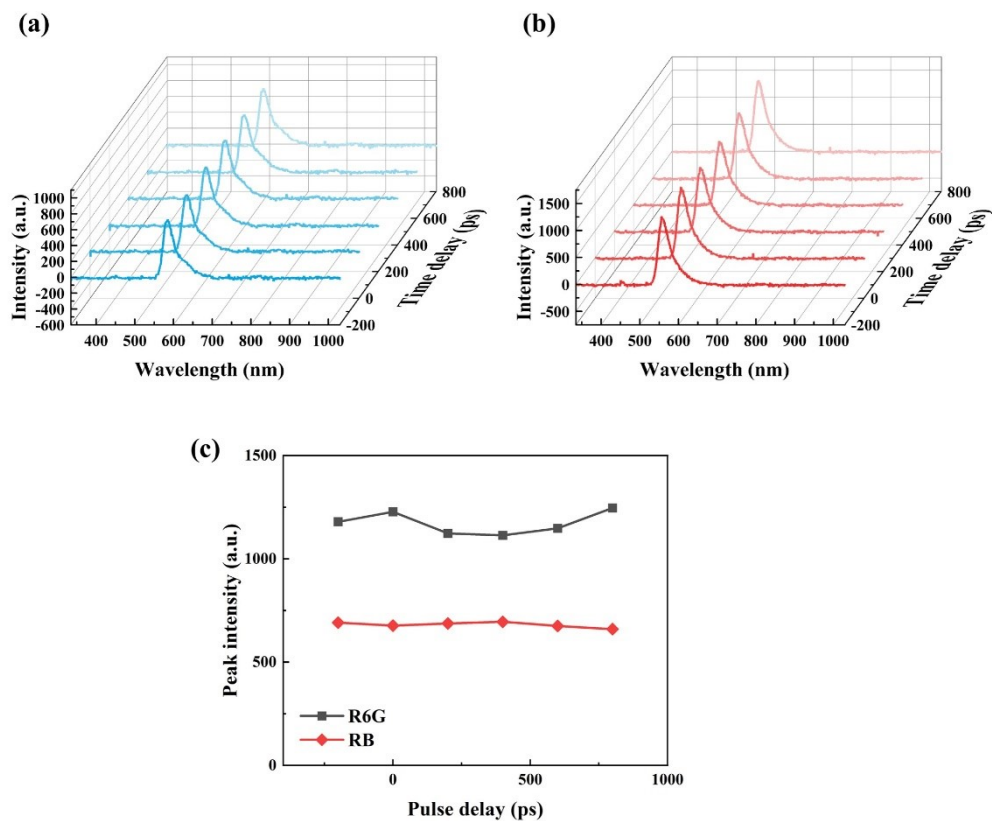


Figure S3. The emission spectra of femtosecond laser induced fluorescence emission in (a) R6G and (b) RB solution, at different time delay. (c) The relationship between peak intensity and the time delay. The power of 800 nm fs laser which was used to generate cavitation bubbles was 20 mW. The time delay is the time between the arrival of each 400 nm and 800 nm laser pulse. The time delay is tuned by the optical delay line.

3. Femtosecond laser induced cavitation bubbles and their influence on optical fields

3.1 Time resolved imaging of femtosecond laser cavitation process

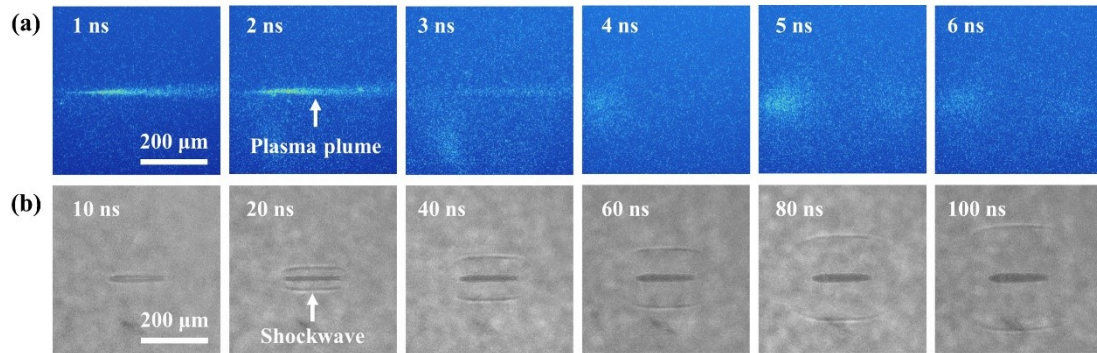


Figure S4. (a) The ICCD images of femtosecond laser induced plasma from 1 to 6 ns after laser irradiation. The exposure time was set to be 1 ns. (b) The ICCD images of shockwave generated from 10 to 100 ns after laser irradiation. The exposure time was set to be 5 ns. All the images were taken after the interaction of an 800 nm femtosecond laser pulse with pulse energy of 20 μJ . The laser pulses were focused 1 mm away from the wall of container.

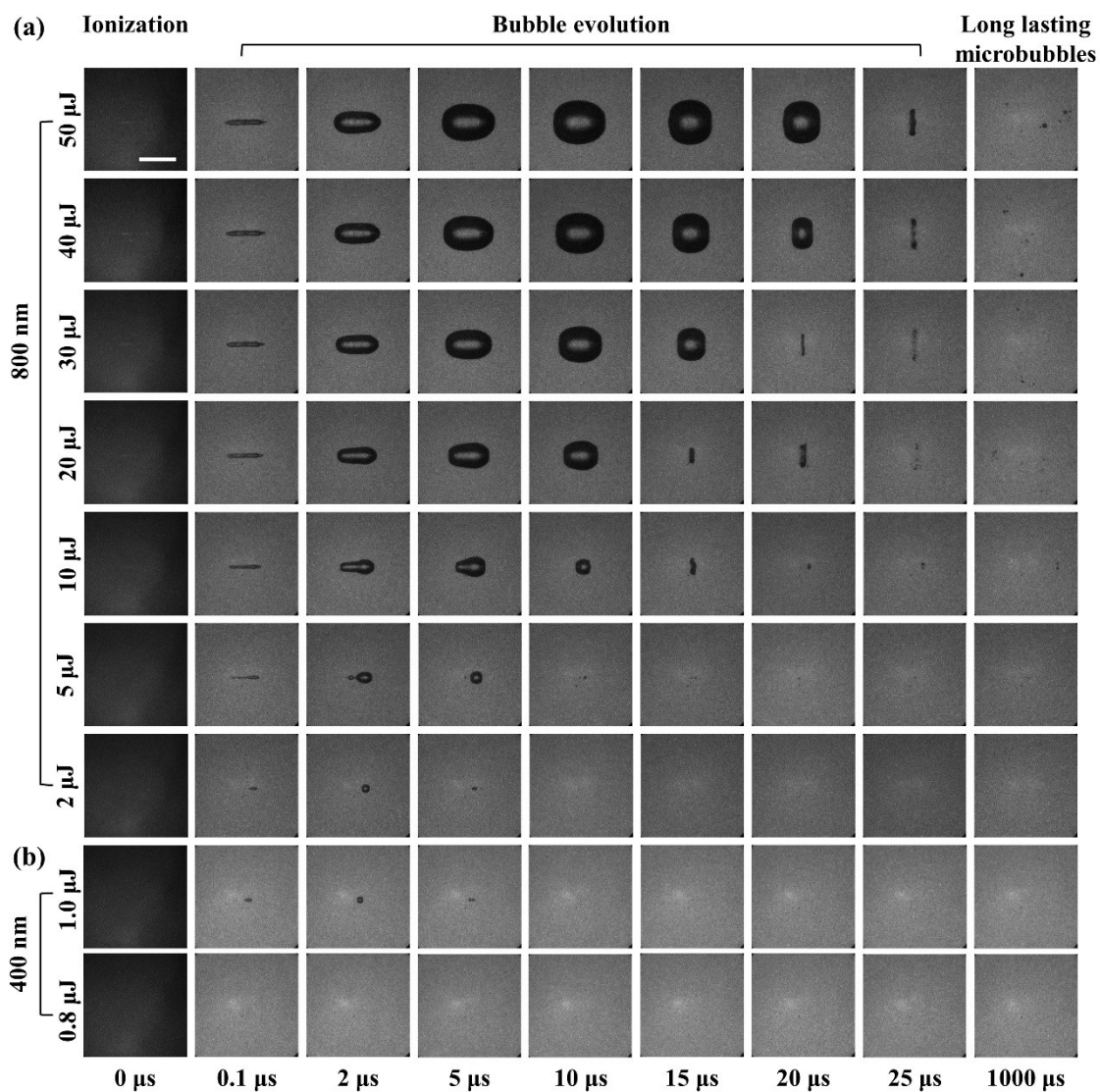


Figure S5. (a) The time-resolved images of 800 nm femtosecond laser induced bubble generation with different pulse energy. **(b)** The time-resolved images of 400 nm femtosecond laser induced bubble generation with different pulse energy. The femtosecond laser pulses were focused 1 mm away from the wall of container by a 50x objective (NA 0.5). The scale bar is 200 μm .

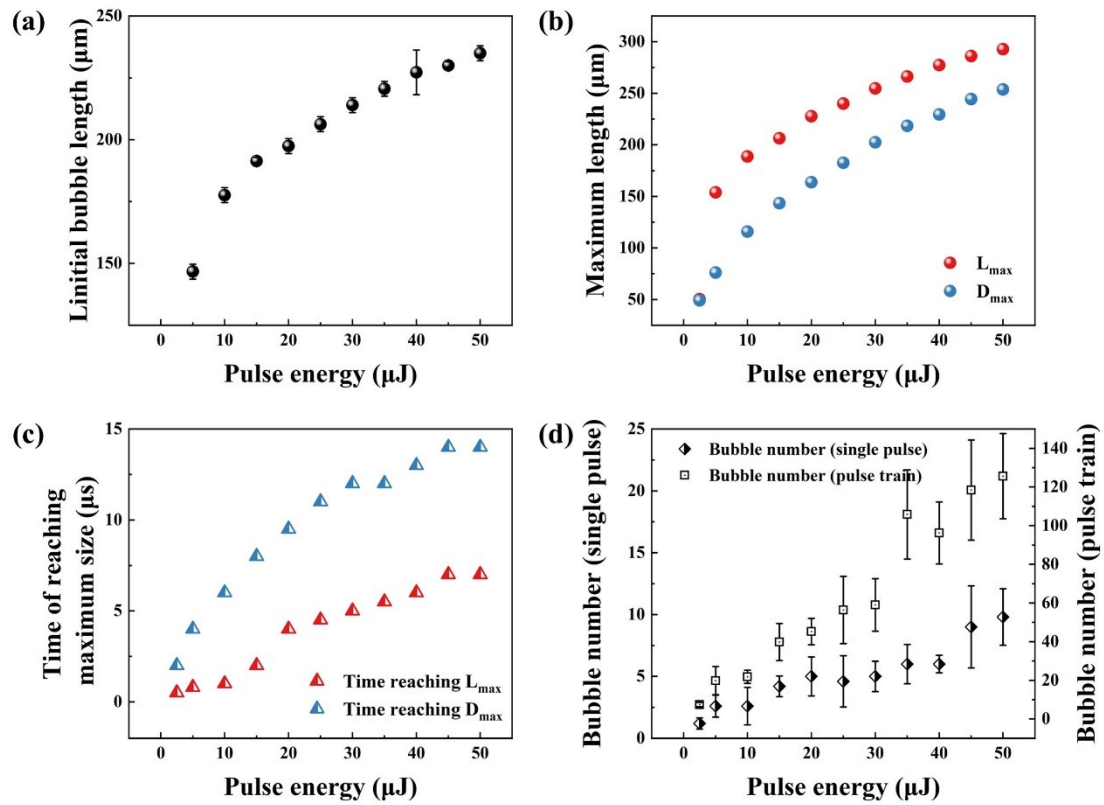


Figure S6. The relationship between bubble cavitation and laser parameters. **(a)** The initial bubble length as a function of pulse energy. **(b)** The maximum bubble size as a function of pulse energy. **(c)** The time of reaching the maximum size as a function of pulse energy. **(d)** The number of long lasting micro bubbles generated by single pulse and continuous pulse train as a function of pulse energy. The bubble number (pulse train) stands for the average number of existing bubbles in the field of view when a 1 kHz pulse train was continuously applied.

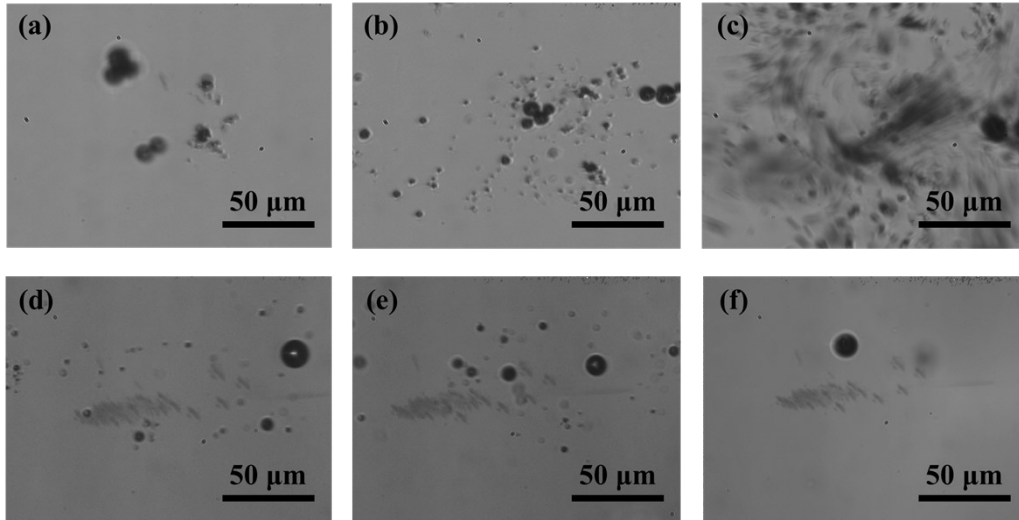


Figure S7. The CCD images of cavitation bubble generation using continuous pulse train. The pulse repetition rate is 1 kHz. The laser pulses were focused 1 mm away from the wall of container. **(a)–(c)** The cavitation bubble induced by ultrafast laser with different pulse energy. The pulse energy is 5 μJ in **(a)**, 20 μJ in **(b)** and 40 μJ in **(c)**. **(d)–(f)** The cavitation bubble at different position. The images were taken at 0 μm in **(d)**, 20 μm in **(e)** and 60 μm in **(f)** away from the focus point. The pulse energy is 20 μJ .

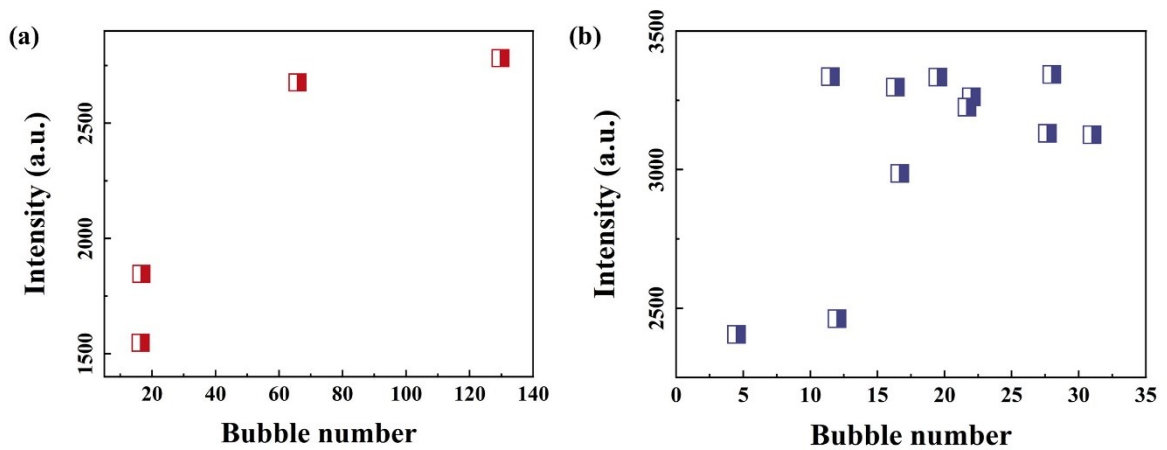


Figure S8. The scatter diagram comparing the bubble number and the emission intensity derived from **Figure 3**. The bubble number is controlled by the 800 nm laser intensity in **(a)** and the position of focus in **(b)**.

3.1 Simulation of optical field enhancement by cavitation bubbles

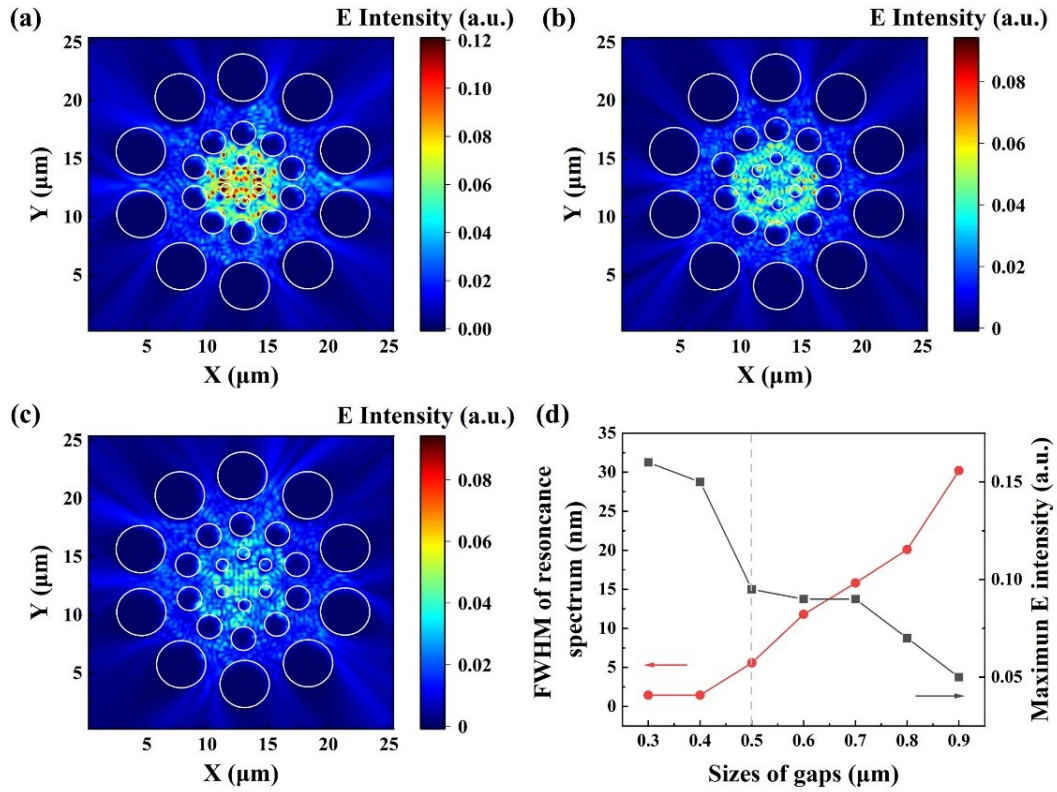


Figure S9. (a)–(c) The simulation results of the optical field intensity around bubble clusters. The gaps between the inner circle bubbles were set to be $0.4 \mu\text{m}$ in (a) and $0.6 \mu\text{m}$ in (b) and $0.8 \mu\text{m}$ in (c). (d) The maximum E intensity and FWHM of resonance spectra as a function of sizes of gaps.

4. Applications of bubble enhanced fluorescence in bio imaging

4.1 The illumination by bubble enhanced fluorescence through scattering medium

Scattering medium is commonly seen in bio tissues and other materials. In the method of cavitation bubble enhanced fluorescence, the light source is generated inside the solution. The influence of the scattering substrate can be avoided. In our experimental condition, the protein crystals are blocked by a layer of spontaneously nucleated crystals at the bottom of the well plates. Direct illumination will be scattered and may result in speckle patterns when coherent light source is applied. **Figure S10** compares the imaging of protein crystals using bubble enhanced fluorescence and directly illuminated by 800 nm ultrafast laser.

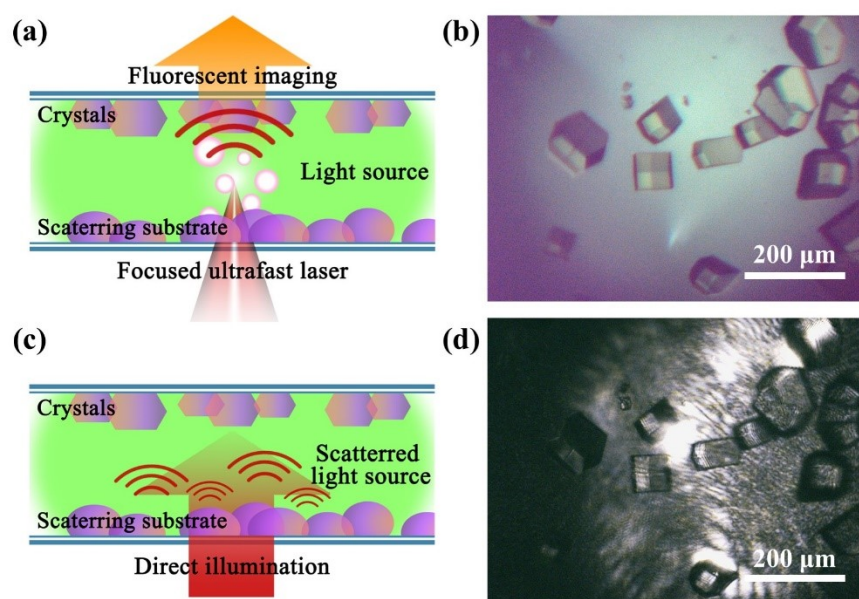


Figure S10. (a)(b) The schematic and the imaging results of protein crystals illuminated by bubble enhanced fluorescence. (c)(d) The schematic and the imaging results of protein crystals illuminated by 800 nm ultrafast laser.

4.2 Applications of bubble enhanced fluorescence in cell imaging

Except for protein crystals, the fluorescence enhancement using femtosecond laser induced cavitation bubbles can be extended to other applications such as the imaging of cells. Cancer cells in the culture solution was used as the imaging objects. The optical path setup was the same as that used in the imaging of protein crystals. The culture solution was composed of glucose, amino acid, pyruvic acid, serum, phenol red, etc. The R6G solution was added into the solution for fluorescence emission. The cancer cells were cultured on the wall of the container. Femtosecond laser was focused into the solution 1 mm above the wall. Fluorescence emission could be observed as shown in **Figure S11**. No cell apoptosis could be observed during and after the laser irradiation. The fluorescence intensity increases with the increase of excitation laser power. Note that the emission spectra were different from that of R6G solution due to the emission of other compounds in the culture solution.

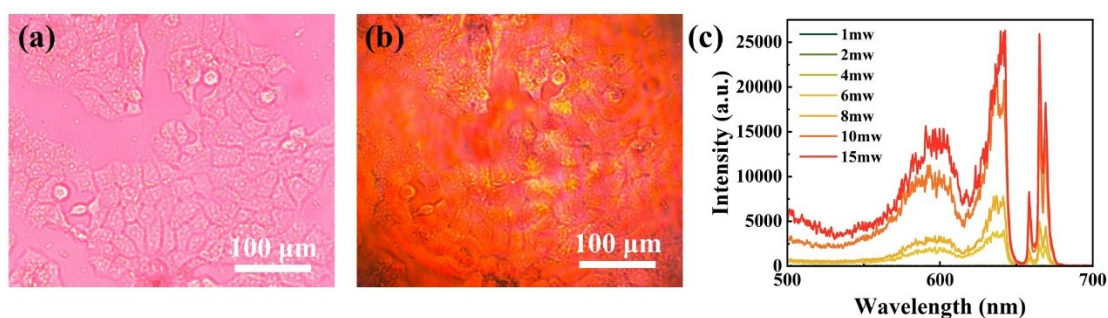


Figure S11. (a) The bright field microscopy and (b) the bubble enhanced fluorescence of cancer cells in culture solution. No cell apoptosis could be observed during and after the laser irradiation. (c) The emission intensity of bubble enhanced fluorescence increase with the increase of excitation laser power. The 800 nm excitation laser passes through the BBO and contains both the 800 nm and 400 nm components.